Supporting Material for:

Elasticity Maps of Living Neurons Measured by Combined Fluorescence and Atomic Force Microscopy

Elise Spedden*†, James D. White*†‡, Elena N. Naumova §, David L. Kaplan‡, Cristian Staii*†

* Department of Physics and Astronomy, Tufts University, †Center for Nanoscopic Physics, Tufts University, 4 Colby St, Medford, MA, USA; ‡Department of Biomedical Engineering, and Department of Chemical Engineering, Tufts University 4 Colby St, Medford, MA, USA, § Department of Civil and Environmental Engineering, Tufts University, 200 College Avenue, Medford, MA, USA

Text S1:

Dorsal root ganglia were surgically isolated from day 9 chick embryos and placed in Hanks Balanced Salt Solution (Life Technologies). The ganglia were incubated in 0.25% Trypsin (Life Technologies) for 30 minutes at 37°C, centrifuged, and the cell pellet was re-suspended in Dulbecco's Minimum Essential Media (Life Technologies) (high glucose supplemented with GlutaMAX (Life Technologies), penicillin/streptomycin (pen/strep) (Life Technologies) 1%, and fetal bovine serum (FBS) (Life Technologies) (2%)). The cells were mechanically dissociated and the suspended cells were added to a cell culture dish, and incubated for 30 minutes allowing adsorption of astrocytes to the dish surface. The remaining media containing neurons was removed. The cells were counted, plated at 200,000 cells per 3.5 cm culture disk, and grown for 4 days.

Rat cortices were obtained from embryonic day 18 rats (Tufts Medical School). The corticies were incubated in 5 mL of trypsin at 37ºC for 20 minutes, then the trypsin was inhibited with 10 mL of neurobasal medium (Life Technologies) supplemented with GlutaMAX, b27 (Life Technologies), and pen/strep, containing 10 mg of soybean trypsin inhibitor (Life Technologies). The neurons were then mechanically dissociated, centrifuged, the supernatant removed, and the cells were resuspended in 20 mL of neurobasal medium containing L-glutamate (Sigma-Aldrich, St. Louis, MO**)**. The neurobasal media was implemented to support neuronal growth without the use of serum, thereby reducing glial cell proliferation. The cells were re-dispersed with a pipette, counted, and plated at a density of 250,000 cells per 3.5 cm culture disk.

P-19 mouse teratocarcinoma stem cells (American Type Culture Collection, Manassas, VA) were cultured using αMinimum Essential Media (Life Technologies, Grand Island, NY) supplemented with FBS (2%), calf bovine serum (CBS) (7.5%) (Life Technologies), and pen/strep (1%). Differentiation was accomplished by incubating the P-19 cells in ultra-low-adhesion cell culture flasks in the presence of retinoic acid (Sigma-Aldrich, St Louis, MO) (2 μM). After 2 days, cell clumps were mechanically dissociated and re-suspended in fresh medium, also containing 2 μM retinoic acid. On day 5, the cell clusters were mechanically dissociated, and plated in fresh medium at a density of 50,000 cells per 3.5 cm culture disk. After an additional 24 hours, cytosine arabinoside (Sigma-Aldrich) was added to remove any undifferentiated cells. The cells were incubated for a minimum of 3 days.

Text S2:

Before measurement on a new sample, each cantilever was calibrated both in air over cleaned glass (to determine accurate lever sensitivity and spring constant values), and in the sample medium (to determine the new lever sensitivity value in fluid).

The in-fluid calibration was performed by two methods to verify accuracy: a thermal calibration (built in to the MFP3D software) that uses the previously determined spring constant value to extract the new sensitivity value, and a deflection vs. z-movement curve calibration on a clean glass area of the sample free from cells or debris. Generally, the two calibration methods gave consistent results and the calibration was considered accurate.

To verify that all cells to be measured were alive, 10 minutes time lapse videos were taken of each cell set before AFM measurements. A 40x objective was used to optically locate the AFM cantilever above each cell and 16 X 16 μm maps of individual force vs. indentation curves were taken on each cell with a resolution of 1μm between points. To limit energy dissipation due to viscoelastic effects the cantilever z velocity was kept at 2 μm/sec, with a maximum cantilever deflection between 5-10nm. Between 5 and 10 well-adhered cells were mapped for each experimental condition (three cell types: chick DRG, mouse P-19 derived, and rat cortical neurons, three surface coatings for each cell type: PDL, laminin, and fibronectin). To assess adherence, during force map acquisition each cell was monitored visually via the 40x objective to rule out any cells that underwent lateral slipping under the force from the cantilever. Cell edges were determined using height data, with all points not on the cell body excluded.

For force data analysis, highly noisy and poorly fitting curves (generally less than 10% for each force map) were excluded from the data. Based on height information all data on areas outside of the cell body region was also excluded. To verify the implemented MFP3D analysis, several curves on multiple samples were also fitted independently by the authors using the Hertz model equation. In this case, the elastic modulus of a force vs. indentation curve was extracted using Sneddon's modification of the Hertz contact model for a 30^0 conical indenter:

$$F = \frac{E}{(1-\nu^2)} \frac{2\tan(\alpha)}{\pi} \delta^2 \qquad (1)$$

where F is the force, E is the elastic modulus, α is the half-angle of the conical indenter, and δ is the indentation depth. For the Poisson ratio (ν) we use 0.33. For curves that were fitted by both methods (Built-in MFP3D software and by-hand analysis in Origin) the results typically agreed to within 90%.

Table S1: p values for the 1-way ANOVA tests for the effect of surface coating; PDL= Poly-D-lysine, LN= Laminin; FN= Fibronectin. The Top 10%, Middle 30% and Bottom 10% values are defined in the main text (see Materials and Methods). The large p values for the majority of combinations of neuron types, surface coatings and ranges of values for elastic modulus show that the cell stiffness is not significantly affected by the surface coating (see also Figure S2).

	High PDL v LN	High PDL v FN	High LN v FN	Med PDL v LN	Med PDL v FN	Med LN v FN	Low PDL v LN	Low PDL v FN	Low LN v FN
P19	0.79418	0.79312	0.95678	0.74986	0.87033	0.7965	0.91614	0.9067	0.73849
DRG	0.14406	0.72038	0.37745	0.90364	0.04925	0.13952	0.83024	0.3037	0.32164
Cortical	0.18441	0.17243	0.70251	0.93726	0.07685	0.17415	0.3498	0.29583	0.05512

Figure S1:

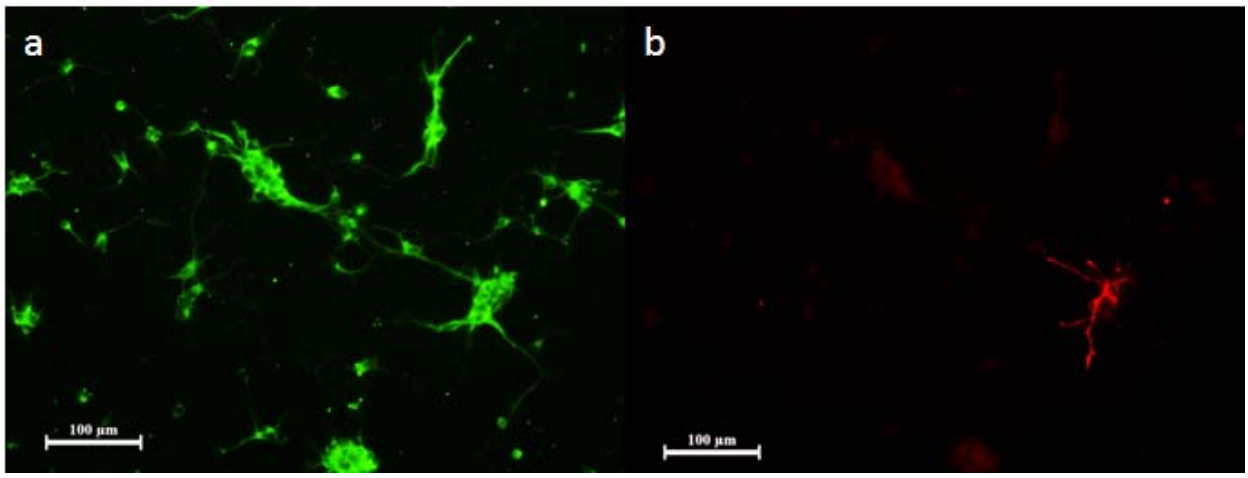

FIGURE S1 Immunostaining experiments on the same region of cortical neuronal cell culture using (a) Anti-β-tubulin III (Sigma Aldrich, St. Louis, MO) diluted 1:500 (neuronal marker) and (b) Anti-Glial Fibrillary Acidic Protein (Sigma Aldrich, St. Louis, MO) (glial cell marker) antibodies. The image indicates cultures of high neuron cell purity. For all measured samples, cortical neurons were further identified via typical morphology. In addition, for all measured DRG neurons we have measured only those cells that display very long processes (≥100µm), which are representative for DRG neurons. P-19 derived neurons were chosen based on morphological similarity to cortical neurons and long processes that do not typically branch. All force maps on P-19 and DRG neurons (Fig 1 and 2 in the main text) were performed on this type of cells, for which all the processes were fully grown (no active growth state was observed on well-developed P-19 and DRGs).

Figure S2:

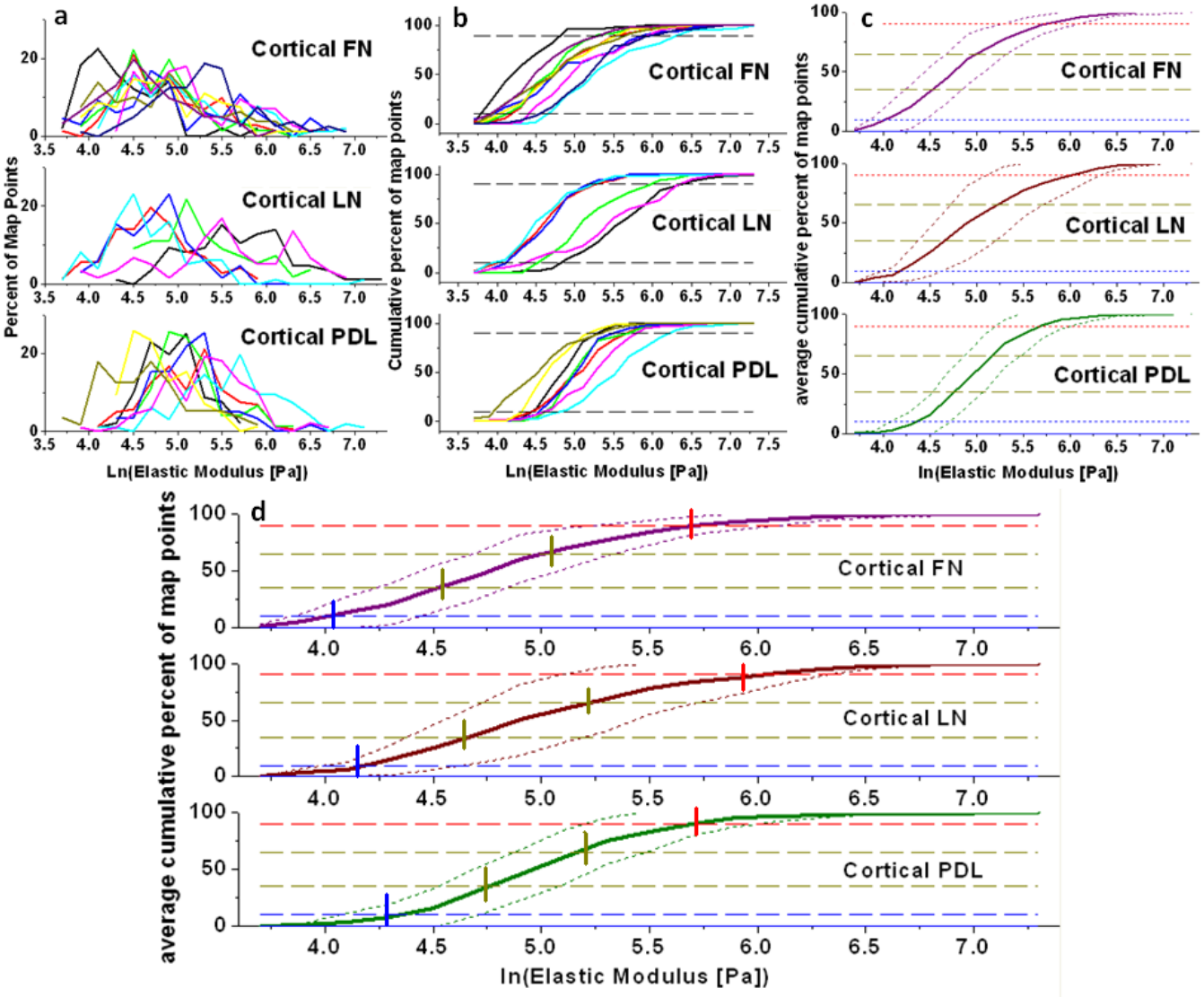

FIGURE S2 (a) Complete individual distributions of map points for the elastic modulus, compiled for each cell, within each surface coating; *top*: fibronectin (FN), *middle*: laminin (LN), *bottom*: poly-D-lysine (PDL). Distributions are displayed as percent of map points within each "bin" plotted vs. the natural log of the measured elastic modulus (Pa) for each bin. To best represent each data set as a distribution, optimal Bayesian binning was applied to log-transformed data. Individual lines represent the distributions from different cells. (b) Cumulative distributions for elastic modulus (i.e. sums of the data points from (a) up to a given bin) vs. the natural log of the measured elastic modulus (Pa) for each bin. Dotted black lines show the cutoff limits for 10^{th} and 90^{th} percentiles, or the top 10% of data and bottom 10% of data, respectively. (c) Average cumulative distributions shown for each surface as the solid line. Dashed yellow lines show the cutoff limits for 35th and 65th percentiles, or the middle 30% of data. Dotted lines

above and below each cumulative distribution illustrate +/- 1 standard deviation (SD) that form a confidence area for each data set. *The confidence areas of cumulative distributions for each surface type overlap along the whole range of values, indicating a very low probability for a surface-dependent effect outside of 1 SD from the average distribution.* (d) Expanded version of the plot shown in (c) with the vertical bold markings indicating the points at which the cumulative average curves cross into or out of the bottom 10% region (blue dashes), the middle 30% region (yellow dashes), or the top 10% region (red dashes). The good level of vertical alignment between these cross points indicates that it is appropriate to use the top 10%, middle 30% and lowest 10% areas as representative of those regions of the data. Similar results are obtained for cumulative distributions calculated for P-19 and DRG cells cultured respectively on FN, LN and PDL coated glass surfaces.

Figure S3:

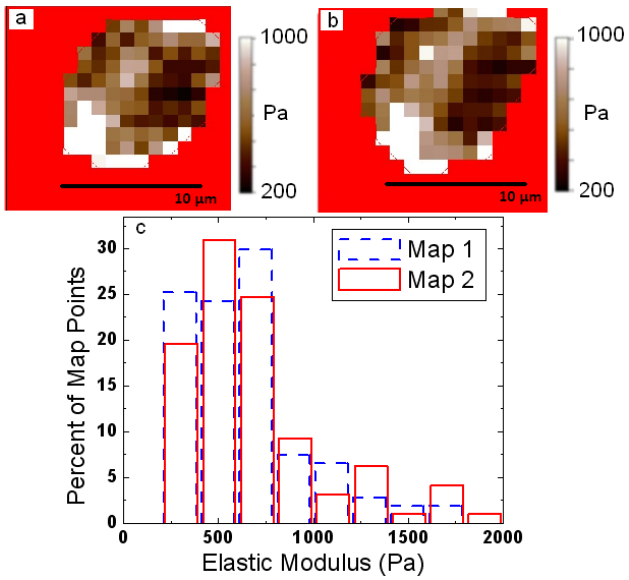

FIGURE S3 (a) Elasticity map of unmodified live cortical cell not undergoing active neurite extension. Histogram of percent of map points in each elastic modulus bin shown in (c) (blue dash). (b) Subsequent elasticity map of the same cell as shown in (a), in the same conditions (no active neurite extension, no chemical modification) taken after 45 min. Histogram of percent of map points in each elastic modulus bin shown in (c) (red solid). Average elastic modulus values between maps (a, b) differ by only 6.5%. Similar results were obtained in 5 other live unmodified cells with no active neurite extension, and with maps taken between 20 minutes and 2 hours apart. The differences in average elastic modulus values obtained from these maps range between a minimum of 3% and a maximum of 14%.

Figure S4:

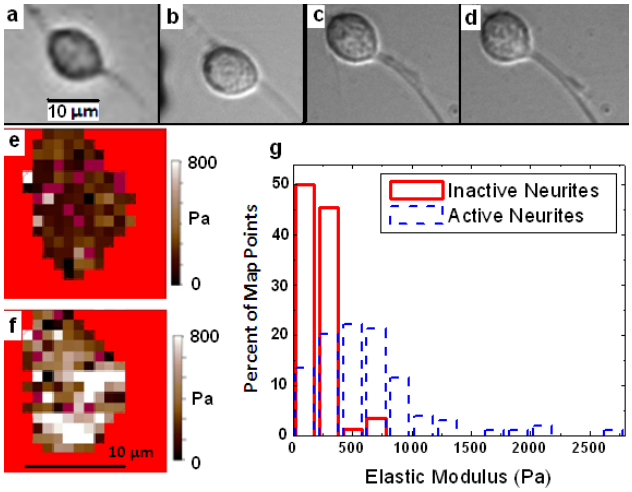

FIGURE S4 (a, b) Optical images before (a) and after (b) force measurements of a live cortical neuron *not undergoing* active neurite extension during 15 minute force-map (passive phase). (c, d) Optical images before (c) and after (d) force measurements of same live cortical neuron at a later time actively undergoing neurite extension (active phase), seen as an increase in the length of the newly visible neurite in the lower right. Scale bar shown in (a) is the same for all images (a-d). (e) Elasticity map for the passive phase shown in (a-b). (f) Elasticity map for the active extension phase shown in (c-d). Scale bar shown in (e) is the same for both maps. g) Histogram of percent of total map points in each elastic modulus bin (see Materials and Methods). Dashed line: data for active extension state. Solid line: data for the passive state. The average elastic modulus value increases by 175% during growth. For all cases where neurons display active neurite extension, we *always* measure an increase in stiffness in those regions of the cells located in the proximity of the active neurite. The combined data from these regions for all (N=5) cells, accounts in average for more than 75% of the overall increase in the stiffness of the cell body observed during growth (and could be up 90% of the overall increase for some individual cells, as shown in Fig S4 *e*, *f*). The data for all cells (N=5) shows that the stiffening of the cell regions close to active neurites is the primary effect that accounts for the overall increase in cell stiffness. However, we also find other regions of the cell that stiffen during the growth phase (shown for example in Fig. 3 *e*). The contribution of these regions to the overall increase in stiffness is typically less than 25%.

Figure S5:

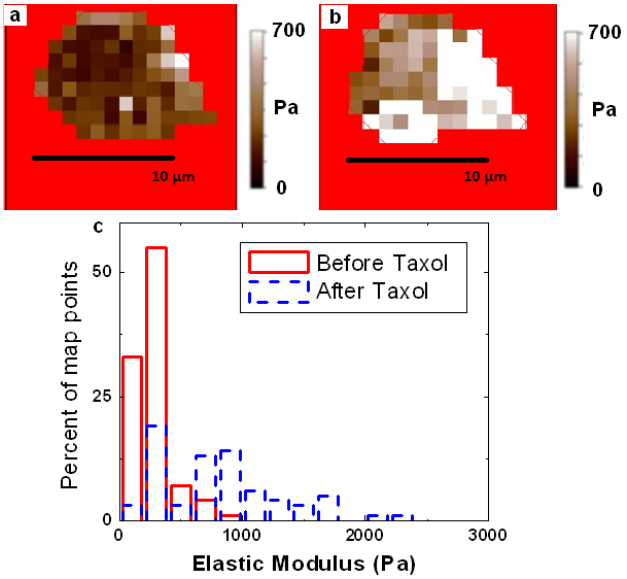

FIGURE S5 (a) Elasticity map of a live cortical neuron, which is not undergoing neurite extension. (b) Elasticity map of the same cell as in (a) shown 90 minutes after addition of 10 µM Taxol. Scale bar is the same for (a) and (b). (c) Histogram of percent of map points in each elastic modulus bin (see Materials and Methods) for the maps shown in (a) (solid line) and (b) (dashed line). Scale bar same for both maps. The average elastic modulus value increases by 180% after the addition of Taxol. Similar results seen on 3 additional cells.

Figure S6:

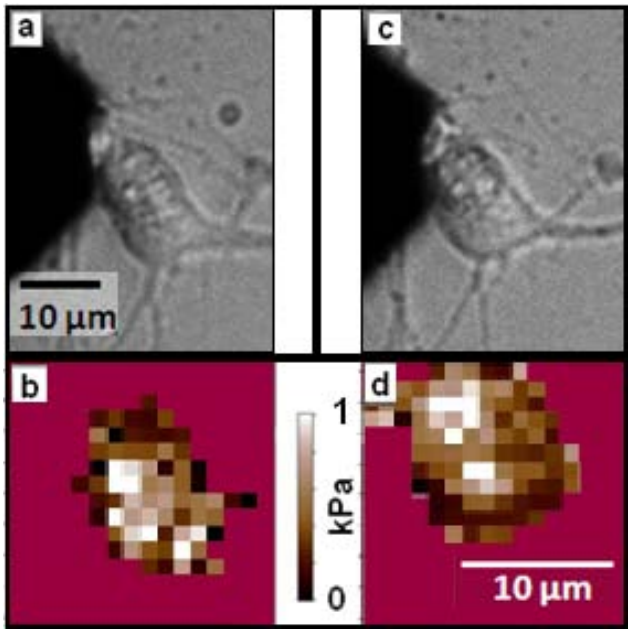

FIGURE S6 (a) Optical image of live cortical cell. (b) Elasticity map of cell shown in (a). (c) Optical image of same cell shown in (a) after application of 10 nM Nocodazole (Sigma-Aldrich, St. Louis, MO). (d) Elasticity map of cell post-Nocodazole showing no appreciable change in overall cell stiffness. Similar results were seen on 1 other treated cell. Additional treated cells (6 out of 8) died before the acquisition of a second force map.

Figure S7:

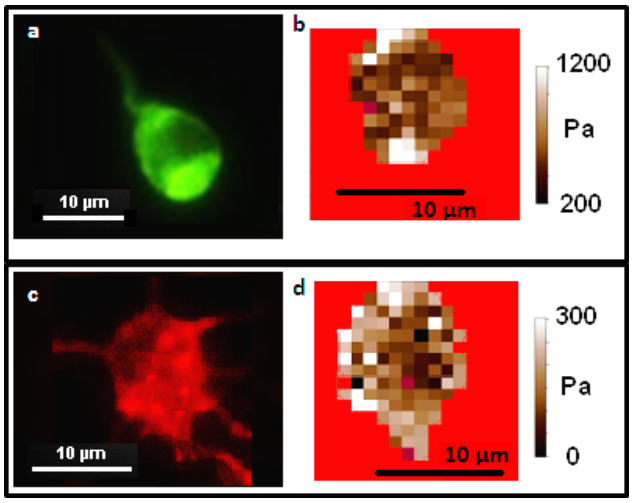

FIGURE S7 (a) FITC fluorescence image of live cortical cell stained for microtubules with 50nM Tubulin Tracker Green. (b) Elasticity map of cell shown in (a). The cell regions with high microtubule concentration (bright areas) in (a) correspond to the high stiffness regions shown in (b). Similar correlations were obtained for 5 additional cells. (c) Texas Red fluorescence image of cortical cell after being fixed and stained for F-actin with Alexa Fluor® 564 Phalloidin. (d) Elasticity map of cell shown in (c) prior to fixing. There is no correlation between the cell regions with high actin concentration (bright regions in (c)) and the cell regions that display high stiffness in (d).

Figure S8:

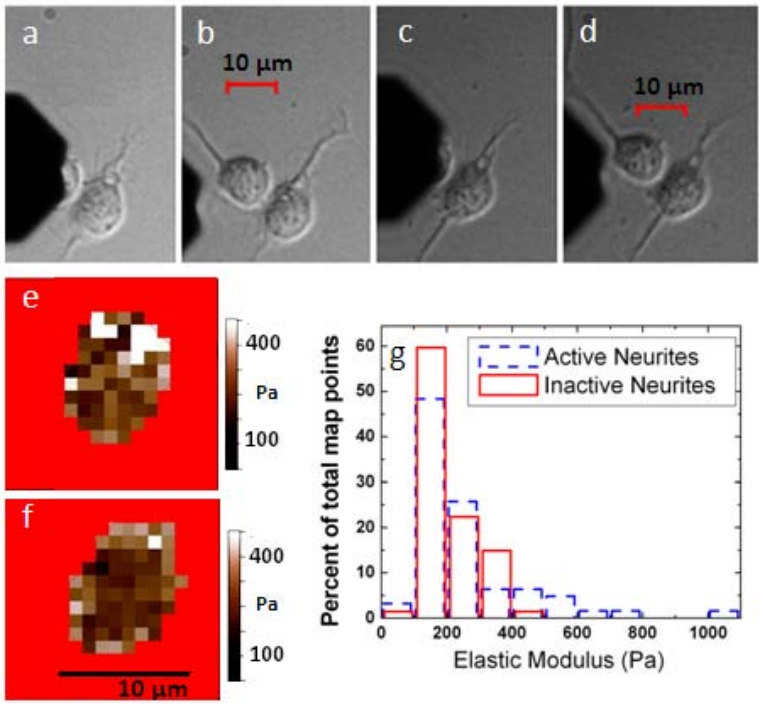

FIGURE S8 (a, b) Optical images before (a) and after (b) force measurements of a live cortical neuron undergoing active neurite extension during 15 minute force-map (*active phase*: seen as an increase in length of the extending top neurite). All measurements were performed in media containing 10 µM Blebbistatin) (c, d) Optical images before (c) and after (d) force measurements of same live cortical neuron (in media containing 10 µM Blebbistatin) at a later time *not undergoing* neurite extension (*passive phase*). Scale bar same for (a), (b), and same for (c), (d). (e) Elasticity map for the active extension phase shown in (a-b). (f) Elasticity map for the passive phase shown in (c-d). Scale bar shown in (f) is the same for both maps. g) Histogram of percent of total map points in each elastic modulus bin (see Materials and Methods). Dashed line: data for active extension state. Solid line: data for the passive state. Similar results were obtained for 2 additional cells. The results show a measured 30-55% increase in stiffness due to growth, which is a similar change to that seen in the majority of growing samples without Blebbistatin.

Figure S9:

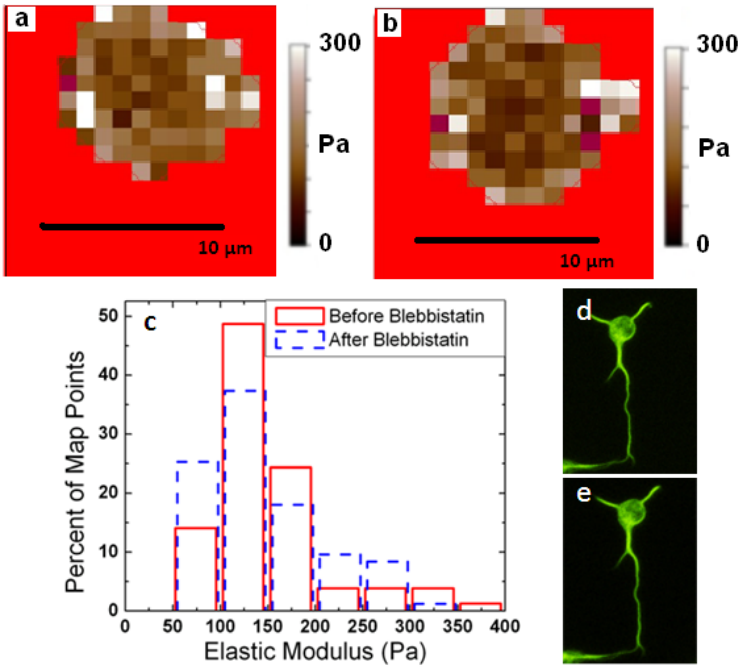

FIGURE S9 (a) Elasticity map of a live cortical neuron. (b) Elasticity map of the same cell as in (a) shown after application of 10 µM Blebbistatin. Scale bar is the same for (a) and (b). (c) Histogram of percent of map points in each elastic modulus bin (see Materials and Methods) for the maps shown in (a) (solid line) and (b) (dashed line). Scale bar same for both maps. Average elastic modulus values between maps (a, b) differ by only 3% indicating no baseline change in stiffness due to application of Blebbistatin. Similar results obtained from 2 additional cells. (d) FITC fluorescence image of live cortical cell (different cell from (a), (b)) stained for microtubules with 50nM Tubulin Tracker Green. (e) Fluorescence image of same cell as in (d) 30 minutes after application of 10 µM Blebbistatin indicating no change in tubulin aggregation after application of Blebbistatin.